General Disclaimer

One or more of the Following Statements may affect this Document

- This document has been reproduced from the best copy furnished by the organizational source. It is being released in the interest of making available as much information as possible.

- This document may contain data, which exceeds the sheet parameters. It was furnished in this condition by the organizational source and is the best copy available.

- This document may contain tone-on-tone or color graphs, charts and/or pictures, which have been reproduced in black and white.

- This document is paginated as submitted by the original source.

- Portions of this document are not fully legible due to the historical nature of some of the material. However, it is the best reproduction available from the original submission.

NASA CR-135248

ANALYSIS OF DELAMINATION IN UNIDIRECTIONAL AND CROSSPLIED FIBER-COMPOSITES CONTAINING SURFACE CRACKS

by
S.S. Wang and J.F. Mandell

MASSACHUSETTS INSTITUTE OF TECHNOLOGY

prepared for

NATIONAL AERONAUTICS AND SPACE ADMINISTRATION

NASA Lewis Research Center
GRANT NSG 3044

1. Report No.	2. Government Accession No.	3. Recipient's Catalog No.
NASA CR 135248		

4. Title and Subtitle	5. Report Date
Analysis of Delamination In Unidirectional and Crossplied Fiber Composites Containing Surface Cracks	May, 1977
	6. Performing Organization Code

7. Author(s)	8. Performing Organization Report No.
S. S. Wang and J. F. Mandell	
	10. Work Unit No.

9. Performing Organization Name and Address	11. Contract or Grant No.
Massachusetts Institute of Technology Cambridge, MA 02139	NSG 3044
	13. Type of Report and Period Covered
12. Sponsoring Agency Name and Address	Interim Report
National Aeronautics and Space Administration Washington, DC 20546	14. Sponsoring Agency Code

15. Supplementary Notes

Project Manager, C. C. Chamis
Materials and Structures Division
NASA Lewis Research Center
Cleveland, OH 44135

16. Abstract

A two-dimensional hybrid stress finite element analysis is described which has been used to study the local stress field around delamination cracks in composite materials. The analysis employs a crack tip singularity element which is embedded in a matrix interlayer between plies of the laminate. Results are given for a unidirectional graphite/epoxy laminate containing a delamination emanating from a surface crack through the outside ply. The results illustrate several aspects of delamination cracks: (1) the localization of the singular stress domain within the interlayer, (2) the local concentration of stress in the ply adjacent to the crack, (3) the nature of the transverse normal and interlaminar shear stress distributions, and (4) the relative magnitudes of K_I and K_{II} associated with the delamination. A simple example of the use of the analysis in predicting delamination crack growth is demonstrated for a glass/epoxy laminate. The comparisons with experimental data show good agreement.

17. Key Words (Suggested by Author(s))	18. Distribution Statement
Fiber composites; Delamination; Stress concentration; Stress analysis; Crack propagation; Hybrid stress finite element	Unclassified

19. Security Classif. (of this report)	20. Security Classif. (of this page)	21. No. of Pages	22. Price*
Unclassified	Unclassified	31	3.75

*For sale by the National Technical Information Service, Springfield, Virginia 22151

FOREWORD

This report describes a portion of the analytical and experimental work for the period 1 May, 1976 through 30 April, 1977. The study was conducted for the NASA-Lewis Research Center by members of the Department of Materials Science and Engineering at the Massachusetts Institute of Technology. The Principal Investigator of the overall program is Prof. F.J. McGarry; other major participants are S.S. Wang and J.F. Mandell. The NASA-LeRC Project Manager is Dr. C.C. Chamis, Mail Stop 49-3.

Efforts in this program are primarily directed towards the development of finite element analyses for the study of flaw growth and fracture of fiber composites. The work described in this report is meant to complement the development of a three-dimensional analysis capability, as well as to advance general understanding of the subject.

ABSTRACT

A two-dimensional hybrid stress finite elment analysis is described which has been used to study the local stress field around delamination cracks in composite materials. The analysis employs a special crack tip element which is embedded in a matrix interlayer between plies of the laminat Results are given for a unidirectional graphite/epoxy laminate containing a delamination emanating from a surface crack through the outside ply. The results illustrate several aspects of delamination cracks: (1) the localization of the singular stress domain within the interlayer, (2) the local concentration of stress in the ply adjacent to the crack, (3) the nature of the transverse normal and interlaminar shear stress distributio s, and (4) the relative magnitudes of K_I and K_{II} associated with the delaminati A simple example of the use of the analysis in predicting delamination crack growth is demonstrated for a glass/epoxy laminate. The comparisons with experimental data show good agreement.

CONTENTS

INTRODUCTION

This paper is concerned with the analysis of delamination cracks propagating between the plies of fiber reinforced composite laminates. This general class of problems has been of concern throughout the history of laminated materials for the obvious reason that the bonding between plies is commonly the element of the material system which is the softest, weakest and most prone to environmental attack. In the case of fiber reinforced plastics, to which this paper is specifically addressed, delamination problems have been of concern from some of the first applications involving the unwinding of missile casings and pipes, to current difficulties with delamination-induced failures in aircraft structures.

Analyses of delamination-type problems have taken the form of very approximate predictions of strength [1,2] and damage extension rates [3] or else more rigorous solutions for very simplified models [4,5]. A full understanding of such problems requires an accurate solution for the local stress distribution in the interply region which takes into account the true geometric and material variables and structural parameters. The analysis described in this paper is intended to provide an accurate numerical solution for a more representative model than those previously used.

MECHANICAL MODEL AND ASSUMPTIONS

The geometry of the problem involves a crack situated between plies which typically have fibers oriented in different directions. Each ply is actually heterogeneous, consisting of fiber and matrix regions, and there may be a matrix-rich region betwen plies. Figure 1 shows a micrograph of a

graphite/epoxy composite containing interply matrix regions which are particularly prominent; other composites may have less identifiable interply regions depending upon the materials and fabrication methods. The mechanical model used in the present analysis assumes that the individual plies are homogeneous and anisotropic, and includes isotropic interply matrix regions (interlayers) between each ply. The interlayers may vary in thickness, but are generally on the order of 1/10 to 1/20 of the ply thickness, similar to Figure 1. The crack tip is embedded in the matrix interlayer as indicated in Figure 2. Linear elastic behavior is assumed for the plies and for the interlayers.

The crack geometries considered in the present study are similar to that in Figure 2. A surface crack is assumed to penetrate one or more plies, initiating the delamination crack. The remainder of the compsosite is assumed to be well bonded and defect-free.

METHOD OF ANALYSIS

General Formulation

The hybrid stress approach of the finite element method, pioneered by Pain [6,7], is characterized by the use of an assumed stress field in the element and an assumed displacement field along the element boundaries. The formulation of the analysis is based on the minimum complementary energy principle (a modified complementary energy functional is used in the formulation of the crack tip superelement). Additional features of the method are flexibility of formulation, selection of elements and expedient achievement of interelement compatibility. More accurate solutions and faster convergence rates than those of conventional displacement models can be obtained. The singular behavior of the crack tip region, which is critical to the fracture problem, can be exactly modeled in the fromulation without an increase in the number of elements. The complex geometric variables and multiphase materials effects also are conveniently taken into account.

The hybrid stress finite lement method procedure is specialized for application to the current plane crack problem by the introduction of a crack tip superelement within which the singular stress behavior is considered by properly selected stress functions. This assumed stress hybrid model for the problem was first introduced by Pian, [6], and later refined by Tong et al [8] by the use of the complex variable formulation of the Muskhelishvili stress function. The general formulation of the procedure is given here for the case of the plane crack

problem in a composite laminate with the superelement embedded in the interlayer. The formulations for the crack tip super-element and its surrounding regular (non-singular) hybrid elements have been described in detail elsewhere [6,8], and only a brief outline is given here.

Consider a crack system of the type shown in Figure 2. The complementary energy functional of the whole domain of the specimen (after division into a finite number of discrete elements) may be expressed as

$$\Pi_c = \Pi_m + \sum_i \Pi_r^{(i)} \tag{1}$$

where π_m is refered to the crack tip superelement and $\pi_r^{(i)}$ to the i^{th} regular surrounding element in the given domain. Applying the variational energy principle to the functional π_c, one obtains

$$\Pi_c = \sum_n \left[\frac{1}{2} \underset{\sim}{q}_n^T \underset{\sim}{K}_n \underset{\sim}{q}_n - \underset{\sim}{q}_n^T \underset{\sim}{\bar{Q}}_n \right] \tag{2}$$

where

$$\underset{\sim}{K}_n = \underset{\sim}{G}_n^T \underset{\sim}{H}_n^{-1} \underset{\sim}{G}_n$$

represents the general form of the element stiffness matrix, and is calculated in different ways in the crack tip superelement and the surrounding regular elements as decribed in the next section. The equivalent nodal force $\underset{\sim}{\bar{Q}}_n$ is defined as

$$\underset{\sim}{\bar{Q}}_n = \underset{\sim}{G}_n^T \underset{\sim}{\beta}_n \tag{3}$$

The matrices, $\underset{\sim}{G}_n$, $\underset{\sim}{H}_n$ and $\underset{\sim}{\beta}_n$ are defined in following sections in detail.

Assembling all the element stiffness matrices together, a set of linear equations of the form

$$\underset{\sim}{K}\ \underset{\sim}{q} = \underset{\sim}{Q} \tag{4}$$

is established. The displacemnt field can be solved by a standard Gauss-Cholosky elimination scheme

$$\underset{\sim}{q} = \underset{\sim}{K}^{-1}\ \underset{\sim}{Q} \tag{5}$$

The stress parameters $\underset{\sim}{\beta}_n$ for the n^{th} element are then calculated from

$$\underset{\sim}{\beta}_n = \underset{\sim}{H}_n^{-1}\ \underset{\sim}{G}_n\ \underset{\sim}{q}_n \tag{6}$$

The associated stress field at the location (x_p, y_p) of interest can be obtained from

$$\underset{\sim}{\sigma}(x_p, y_p) = \underset{\sim}{P}(x_p, y_p)\ \underset{\sim}{H}_n^{-1}\ \underset{\sim}{G}_n\ \underset{\sim}{b}_n\ \underset{\sim}{q}_n \tag{7}$$

where $\underset{\sim}{b}_n$ is a Boolean transformation.

Crack-Tip Element Formulation

The conventional displacement model and non-singular hybrid stress element have difficulty handling the crack problems even in a monolithic material, since the use of high order polynomials as interpolation

functions does not improve the rate of convergence for this kind of problem. The reason for this is that the convergence rate of the finite element method is controlled by the nature of the solution near the singular region [8]. However, use of the complex variable technique in the hybrid element formulation permits proper consideration of the stress singularity and of higher order effects in the crack tip region, and it leads to highly accurate results with a relatively coarse mesh.

The modified complementary energy functional, π_m, is used for the crack tip element. Consider a plane elasticity problem with prescribed boundary traction $\bar{T}_i$ over the boundary s_σ and prescribed displacement u_i over the boundary s_u. The functional is defined in the form

$$\Pi_m = \int_{\partial A_m} (\tilde{u}_i - u_i) T_i \, ds - \int_{(S_\sigma)_m} u_i \bar{T}_i \, ds + \frac{1}{2} \iint_{A_m} [\sigma_{ij} (u_{i,j} + u_{j,i}) - S_{ijkl} \sigma_{ij} \sigma_{kl}] \, dA \qquad [8]$$

The Euler equations for this functional are

$$\frac{1}{2} (u_{i,j} + u_{j,i}) = S_{ijkl} \sigma_{kl} \qquad [9]$$

$$\sigma_{ij,j} = 0 \qquad [10]$$

Following Muskhelishvili's formulation [9], the stress and displacement fields in the plane elasticity problem can be expressed in terms of two stress functions $\phi(z)$ and $\psi(z)$ of the complex variable z as

$$\begin{aligned} \sigma_{yy} + \sigma_{xx} &= 2 [\phi'(z) + \overline{\phi'(z)}] \\ \sigma_{yy} - \sigma_{xx} + 2i \sigma_{xy} &= 2 [\bar{z} \phi''(z) + \psi'(z)] \end{aligned} \qquad (11)$$

and

$$2G(u+iv) = \eta\phi(z) - z\overline{\phi'(z)} - \overline{\psi(z)}$$

where both $\phi(z)$ and $\psi(z)$ are analytical in the Z-plane, and $G = E/2(1+\nu)$ with

$$\eta = (3-\nu)/(1+\nu) \quad \text{for plane stress} \tag{12}$$

or $$\eta = (3-4\nu) \quad \text{for plane strain} \tag{13}$$

In order to choose proper stresses and displacements for the crack element which would account for possible singularities of all orde., as well as higher order terms, the following mapping function is introduced

$$z = w(\zeta) = \zeta^2 \tag{14}$$

with

$$-\pi/2 \le \arg\zeta \le \pi/2$$

Thus, on the ζ-plane the stress functions $\phi(\zeta)$ and $\psi(\zeta)$ are analytical functions of ζ. Using this mapping function, Eq. (11) becomes

$$\sigma_{yy} + \sigma_{xx} = 4\,\mathrm{Re}[\phi'(\zeta)/w'(\zeta)]$$

$$\sigma_{yy} - \sigma_{xx} + 2i\sigma_{xy} = 2\{\overline{w(\zeta)}[\phi'(\zeta)/w'(\zeta)]' + \psi(\zeta)\}/w'(\zeta) \tag{15}$$

and

$$2G(u+iv) = \eta\phi(\zeta) - w(\zeta)\overline{\phi'(\zeta)}/\overline{w'(\zeta)} - \overline{\psi(\zeta)}$$

By imposing the traction free boundary condition ($T_x = T_y = 0$) on the crack surface, as

$$i\int_s (T_x + iT_y)\,ds = 0 = \phi(z) + z\overline{\phi'(z)} + \psi(z) \tag{16}$$

$\psi(\zeta)$ can be calculated from $\phi(\zeta)$

$$\psi(\zeta) = -\overline{\phi(-\bar{\zeta})} - \overline{w(-\bar{\zeta})}\,\phi'(\zeta)/w'(\zeta) \tag{17}$$

In constructing the superelement stiffness matrix, $\phi(\zeta)$ is assumed to have the form

$$\phi(\zeta) = \sum^{N} b_j \zeta^j \tag{18}$$

Thus, from Eq. (17) we have

$$\psi(\zeta) = -\sum^{N} [\bar{b}_j (-1)^j + j\, b_j/2]\, \zeta^j \tag{19}$$

where

$b_j = \beta_j + i\,\beta_{N+j}$ (non-symmetric case)

$b_j = \beta_j$ (symmetric case)

with the β's being real constants.

Substituting Eqs. (18) and (19) back into Eqn. (15), the stresses and displacements can be explicitly expressed in terms of ζ as

$$\sigma_{xx} - i\,\sigma_{xy} = \sum^{N} \left\{ Re\,(j\zeta^{j-2}) - \left[\frac{(j-2)}{4}\frac{\bar{\zeta}^2}{\zeta^2} - \frac{j}{2} - \frac{1}{2}(-1)^j\right] j\zeta^{j-2} \right\} \beta_j$$
$$+ \sum^{N} \left\{ i\,Im\,(j\zeta^{j-2}) - i\left[\frac{(j-2)}{4}\frac{\bar{\zeta}^2}{\zeta^2} - \frac{j}{4} + \frac{1}{2}(-1)^j\right] j\zeta^{j-2} \right\} \beta_{N+j} \tag{20 a,b, and c}$$

$$\sigma_{yy} + i\,\sigma_{xy} = \sum^{N} \left\{ Re\,(j\zeta^{j-2}) + \left[\frac{(j-2)}{4}\frac{\bar{\zeta}^2}{\zeta^2} - \frac{j}{4} - \frac{1}{2}(-1)^j\right] j\zeta^{j-2} \right\} \beta_j$$
$$+ \sum^{N} \left\{ -i\,Im\,(j\zeta^{j-2}) + i\left[\frac{(j-2)}{4}\frac{\bar{\zeta}^2}{\zeta^2} - \frac{j}{4} + \frac{1}{2}(-1)^j\right] j\zeta^{j-2} \right\} \beta_{N+j}$$

$$2G(u+iv) = \sum_{j=1}^{N} \{ [\kappa z^j + (-1)^j \bar{z}^j] - \tfrac{1}{2} j \bar{z}^{j-2} (z^2 - \bar{z}^2) \} \beta_j$$
$$+ i \sum_{j=1}^{N} \{ [\kappa z^j + (-1)^j \bar{z}^j] + \tfrac{1}{2} j \bar{z}^{j-2} (z^2 - \bar{z}^2) \} \beta_{N+j}$$

From Eqs. 20 (a, b, and c) one can express the boundary tractions and interior displacement as

$$\underset{\sim}{T} = \underset{\sim}{R}\, \underset{\sim}{\beta_c} \tag{21}$$

$$\underset{\sim}{u} = \underset{\sim}{U}\, \underset{\sim}{\beta_c}$$

where β_c is a column vector with its components being β_1, β_2, ... β_{2N}. The boundary displacement $\tilde{u}$ shall be assumed in terms of generalized nodal displacement q as

$$\tilde{\underset{\sim}{u}} = \underset{\sim}{L}\, \underset{\sim}{q} \tag{22}$$

A substitution of Eqs. (21) and (22) into Eq. (8) and variation of the functional π_m with respect to $\underset{\sim}{\beta}_c$ yields the crack element stiffness matrix $\underset{\sim}{k}_c$

$$\underset{\sim}{K}_e = \underset{\sim}{G}^T \underset{\sim}{H}^{-1} \underset{\sim}{G} \tag{23}$$

and

$$\underset{\sim}{f} = \underset{\sim}{H}^{-1} \underset{\sim}{G}\, \underset{\sim}{\zeta} \tag{24}$$

where

$$\underset{\sim}{H} = \tfrac{1}{2} \int_{\partial A_m} (\underset{\sim}{U}^T \underset{\sim}{R} + \underset{\sim}{R}^T \underset{\sim}{U})\, ds \quad \text{and} \quad \underset{\sim}{G} = \tfrac{1}{2} \int_{\partial A_m} \underset{\sim}{R}^T \underset{\sim}{L}\, ds$$

After obtaining the displacement field of the system by solving the assembled global stiffness matrix $\underset{\sim}{K}$, the stress field in the super-element can be calculated from Eqns. 20 (a,b and c). The stress intensity factors K_I and K_{II} can be related to $\underset{\sim}{C}_c$ by

$$\begin{bmatrix} K_I \\ K_{II} \end{bmatrix} = \sqrt{2\pi} \begin{bmatrix} \beta_1 \\ \beta_{N+1} \end{bmatrix} \tag{25}$$

Regular Hybrid Stress Element Formulation

The complementary energy functional bo be varied for the regular element is given by

$$\tilde{\Pi}_r^{(m)} = \iint_{A_m} \tfrac{1}{2} \underset{\sim}{\sigma}^T \underset{\sim}{S} \underset{\sim}{\sigma} \, dA - \int_{S_{u_m}} \underset{\sim}{\bar{u}}^T T \, ds \tag{26}$$

where the compliance matrix $\underset{\sim}{S}$ is expressed as

$$\underset{\sim}{S}^{(i)} = \begin{bmatrix} S_{11} & S_{12} & S_{16} \\ S_{21} & S_{22} & S_{26} \\ S_{61} & S_{62} & S_{66} \end{bmatrix}_{(i)}$$

for general i^{th} anisotropic ply of the composite.

Along each boundary of the element, an assumed displacement field is selected, and expressed in terms of the nodal displacements $\underset{\sim}{q}$

$$\underset{\sim}{\bar{u}} = \underset{\sim}{L} \underset{\sim}{q} \tag{27}$$

where $\underset{\sim}{L}$ is the interpolation function. The stresses in the interior of the element are expressed by undetermined stress parameters $\underset{\sim}{\beta}$

$$\underset{\sim}{\sigma} = \underset{\sim}{P}(x,y)\underset{\sim}{\beta} \tag{28}$$

where $\underset{\sim}{P}$ is chosen to satisfy the homogenous equilibrium equation

$$\sigma_{ij,j} = 0 \tag{29}$$

The surface tractions, which are related to the stress components by $T_i = \sigma_{ij} n_j$, can be written in the form

$$\underset{\sim}{T} = \underset{\sim}{R}\underset{\sim}{\beta} \tag{30}$$

Substitution Eqs. (27), (28), and (30) into (26), the functional $\pi_r^{(m)}$ becomes

$$\pi_r^{(m)} = \frac{1}{2}\underset{\sim}{\beta}^T \underset{\sim}{H}\underset{\sim}{\beta} - \underset{\sim}{\beta}^T \underset{\sim}{G}\underset{\sim}{q} \tag{31}$$

where

$$\underset{\sim}{H} = \iint_{A_m} \underset{\sim}{P}^T \underset{\sim}{S}\underset{\sim}{P}\, dA \qquad \text{and} \qquad \underset{\sim}{G} = \int_S \underset{\sim}{R}^T \underset{\sim}{L}\, ds$$

Taking the variation of the functional $\pi_c^{(m)}$ with respect to the stress parameters $\underset{\sim}{\beta}$ to minimize the complementary energy, the element stiffness matrix can be obtained as

$$\underset{\sim}{K}_r = \underset{\sim}{G}^T \underset{\sim}{H}^{-1}\underset{\sim}{G} \tag{32}$$

Accuracy of the Analysis

The accuracy and convergence of the analysis are complicated by several unusual features of the problem and of the crack-tip superelement. As mentioned earlier, the finite element mesh must accommodate both the small dimension of the interlayer thickness and the larger dimensions of the remainder of the specimen, a difference of three orders of magnitude. It is essential to model the interlayer and the crack tip region accurately with a number of elements across the interlayer thickness so that the high stress gradient within the interlayer may be discerned. This geometric characterstic combines with the extreme difference in interlayer and ply elastic modulus to cause significant numerical round-off errors, so double precision mode was required for accurate solutions.

Optimization of the mesh discretization is also complicated by the differences between the crack tip superelement and the surrounding elements. The superelement gives an exact stress distribution, and it is advantageous to use as large a crack tip superelement as possible. On the other hand, the regular elements surrounding the crack tip must be sufficiently small to give accurate results in the domain beyond the superelement, which also is of interest. As a result, a compromise must be reached which yields an accurate solution both very close to the crack tip and in the surrounding region, which also gives the minimum band width for the stiffness matrix. Arrangement of the mesh must also satisfy the geometric contraint that the crack tip superelement be embedded in the interlayer, and that the number of degrees of freedom of the entire system be minimum in terms of computer run time.

A study of the accuracy and convergence of the analysis has been made using test cases for which independent solutions are available in the literature. The test cases studied were double-edge-notched plate and the double cantilever beam type crack geometry. Results described elsewhere [10] indicate excellent agreement with the existing solutions for the test cases. These results, as well as convergence studies for adhesive crack problems similar to the present case, indicate an accuracy within approximately one percent of the converged solution of K_I and K_{II} for mesh arrangements of the type indicated in Figure 2.

RESULTS AND DISCUSSION

Stress Distribution for Unidirectional Laminate

This section gives the stress distribution for a four-ply unidirectional laminate with the fibers parallel to the applied stress. The elastic constants for the plies given in Table 1 are typical of graphite/epoxy. The interlayers between plies have a thickness of one-tenth of the ply thickness and have elastic constants, also given in Table 1, typical of epoxy. The surface crack in this case penetrates through only one ply on the outside, and the delamination crack has a length of three times the ply thickness.

Figure 3 gives an isostress contour plot of the distribution of the longitudinal stress, σ_{xx}, for a section of the laminate around the delamination crack tip. The isostress contours are plotted by the computer and are only approximate, but give an overall view of the nature of the stress field. Several features of the stress field are evident:

1. There is a very localized disturbance in the stress field within the interlayer at the crack tip.

2. There is a local stress concentration in the uncracked adjacent ply just above the delamimation crack tip.

3. The cut ply shows some local compression along the crack flank, and a gradual build up of stress beyond the delamination crack as stress is transferred by shearing of the interlayer.

4. The far-field stresses gradually decrease through the thickness reflecting the bending of the specimen resulting from the nonsymmetry.

The stresses in the interlayer very close to the crack tip are given more accurately on the log-log plot in Figure 4. As expected from previous work on adhesives [10]. The stresses very close to the crack tip follow a $1/\sqrt{r}$ singularity indicated by a slope of -1/2. The associated stress intensity factors, K_I and K_{II}, are $.029\sigma_\infty$ and $.045\sigma_\infty$ respectively. The singular stress domain is completely embedded within the interlayer.

Figure 5 gives linear plots of the variation of σ_{xx} through the thickness at various distances ahead of the crack tip. As before, the severe redistribution of local stress in the ply adjacent to the delamination is evident. It should be noted in Figures 3 and 5 that the domain where σ_{xx} is very high encompasses only a small part of the ply thickness adjacent to the delamination, dropping significantly within several fiber diameters. This suggests that the assumption of homogeneity within the ply may be questionable in this domain. This local stress concentration also preculudes the application of laminate theory.

Figures 6 and 7 present isostress contour and linear plots for the transverse normal stress, σ_{zz}. The distribution of σ_{zz} is centered about the delamination crack tip and is continuous across the ply boundaries. The interlaminar shear stress, σ_{xz}, given in Figures 8 and 9, is more distorted along the fiber direction. σ_{xz} reaches higher values than does σ_{zz} for this case.

The useufulness of the analysis in predicting crack extension depends to a large extent upon the choice of appropriate crack growth criteria. While no attempt has yet been made to select the best criterion for the mixed-mode crack extension, one of the most elementary criteria, the critical total strain energy release rate for composites, has been employed as an example. The critical total strain energy release rate criterion [11] states that crack extension will occur when

$$G_I + G_{II} = G_c \tag{33}$$

This criterion may be expressed in terms of K_I and K_{II} as

$$\left(\frac{K_I}{K_{Ic}}\right)^2 + \left(\frac{K_{II}}{K_{IIc}}\right)^2 = 1 \tag{34}$$

This criterion was applied by obtaining values of K_I and K_{II} for several crack lengths from the computer analysis. The value of applied stress necessary for crack extension was then calculated at each delamination crack length from Eq. (34) and a prediction for the delamination length, ℓ_d, vs. the applied stress, σ_∞, was thus obtained. The composite system chosen for this calculation was Type 1003 glass/epoxy (3M Co.) in the ply configuration 90/0/0/90, due to the availability of experimental data for the delamination crack growth [12] as well as data for G_{Ic} and G_{IIc} for an almost identical material, Type 1002 glass/epoxy [11]. The geometry tested was similar to that in Figure 2 except that two plies were surface cracked, one 90° and one 0°,

giving a surface crack depth of one-half of the total thickness. Since the crack growth occurs in the matrix interlayer, the values of K_{Ic} and K_{IIc} were calculated from G_{Ic} and G_{IIc} by the following equations, using the matrix elastic constants.

$$K_{Ic} = \frac{1}{(1-\nu^2)} (G_{Ic} E_m)^{1/2}$$

$$K_{IIc} = \frac{1}{(1-\nu)} (G_{IIc} G_m)^{1/2}$$

The justification for use of these relationships is discussed elsewhere [10]. Table 1-c lists the values of the various parameters, and Table 1-c gives the elastic moduli for glass/epoxy used in the analysis.

Figure 10 indicates good agreement between calculated and measured delamination crack growth rates under increasing applied stress. The delamination spreads in a stable manner initially due to the decreasing values of K_I and K_{II} with increasing crack length. The applied stress must be increased to promote further crack extension until the delamination becomes long enough such that it propagates under constant stress. The delamination length in Fig. 10 is normalized by w, the experimental specimen width, which was 100 t_o. Since the crack extension is stable, the calculation based on successive crack initiations from different delamination lengths appears to be adequate, without the need for predicting the rate or magnitude of extensions at at each step. The calculated stress values at discreet crack lengths are simply fit by a curve to provide a continuous prediction.

SUMMARY AND CONSLUSIONS

A two-dimensioanl finite element analysis has been developed which gives an accurate solution for the local stress distribution around delamination cracks in laminates. The laminate is modeled as consisting of homogeneous, anisotropic plies separated by an isotropic matrix interlayer. A special superelement is embedded in the interlayer at the crack tip. For the cases studied, the geometry consisted of a strip of material containing a surface crack intersecting a delamination crack.

Sample results for a unidirectional graphite-epoxy laminate illustrate the fundamental aspects of the stress field, including: (1) the localization of the singular stress domain in the interlayer, (2) the very local concentration of stress in the portion of the first continuous ply adjacent to the delamination, (3) the nature of the transverse normal and interlaminar shear stress distributiosn, and (4) the relative magnitudes of K_I and K_{II} associated with the delamination. An example of the prediction of delamination crack growth under increasing applied stress shows good agreement with experimental data.

REFERENCES

1. Kies, J.A. and Bernstein, H., Proc. 17th. Conf. SPI Reinf. Plastics/ Composites Inst., 1962, paper 6-B.

2. Sendeckyj, G.P., Proc. 12th Annual Meeting, Soc. Engr. Sci., Univ. Texas at Austin Press, 1975, p. 625.

3. Im, J., Mandell, J.M., and McGarry, F.J., Proc. 32nd conf., SPI Reinf. Plastics/Composites Inst., 1977, paper 9 F.

4. Willimas, M.L., Bull. Seismolog. Soc. Amer., Vol. 49.

5. Erdogan, F., "Fracture Problems in Composite Materials", NASA-TR-72-2, 1972.

6. Pian, T.H.H., AIAA Journal, 2 (1964) 1333.

7. Pian, T.H.H., and Tong, P., International J. Numerical Methods in Engineering, 1 (1969) 3.

8. Tong, P., Pian,T.H.H., and S.J. Lasry, International J. Numerical Methods in Engineering, 7 (1973), 297.

9. Muskhelishvili, N.I., Some Basic Problems in the Mathematical Theory of Elastic Nordhoff, Groningen, Holland (1953).

10. Wang, S.S., Mandell, J.F. and McGarry, F.J., " Fracture of Adhesive Joints" MIT Dept. Mat. Sci. & Eng. Report 76-1, 1976.

11. Wu, E.M. and Reuter, R.C., "Crack Extension in Fiberglass Reinforced Plastics," TAM Report 275, Univ. of Illinois, 1965.

12. Im, J., Mandell, J.F., Wang, S.S., and McGarry, F.J., "Surface Crack Growth in Fiber Composites", NASA-CR-135094, 1976.

Table 1. Ply Elastic Constants used in Analysis

a. GRAPHITE/EPOXY

E_{LL} = 138. GPa (20.00 x 10^6 psi)

$E_{TT} = E_{ZZ}$ = 14.5 GPa (2.10 x 10^6 psi)

G_{TL} = 5.87 GPa (0.85 x 10^6 psi)

$\nu_{TL} = \nu_{LZ} = \nu_{TZ} = 0.21$

b. FIBERGLASS/EPOXY

E_{LL} = 34.5 GPa (5.00 x 10^6 psi)

$E_{TT} = E_{ZZ}$ = 10.4 GPa (1.50 x 10^6 psi)

G_{LT} = 5.18 GPa (0.75 x 10^6 psi)

$\nu_{TL} = \nu_{LZ} = \nu_{TZ} = 0.25$

c. EPOXY INTERLAYER

E = 3.45 GPa (0.50 x 10^6 psi)

G = 1.28 GPa (0.185 x 10^6 psi)

$\nu = 0.35$

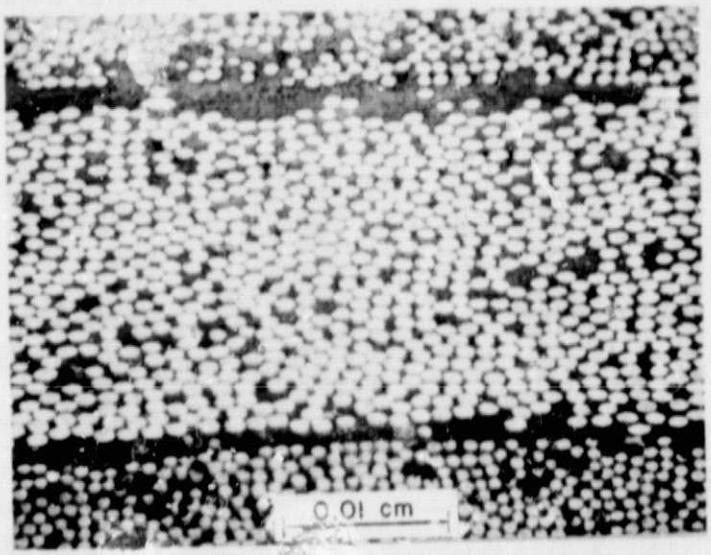

FIGURE 1.

MICROGRAPH OF CROSS-SECTION OF GRAPHITE/EPOXY COMPOSITE SHOWING MATRIX INTERLAYERS BETWEEN PLIES.

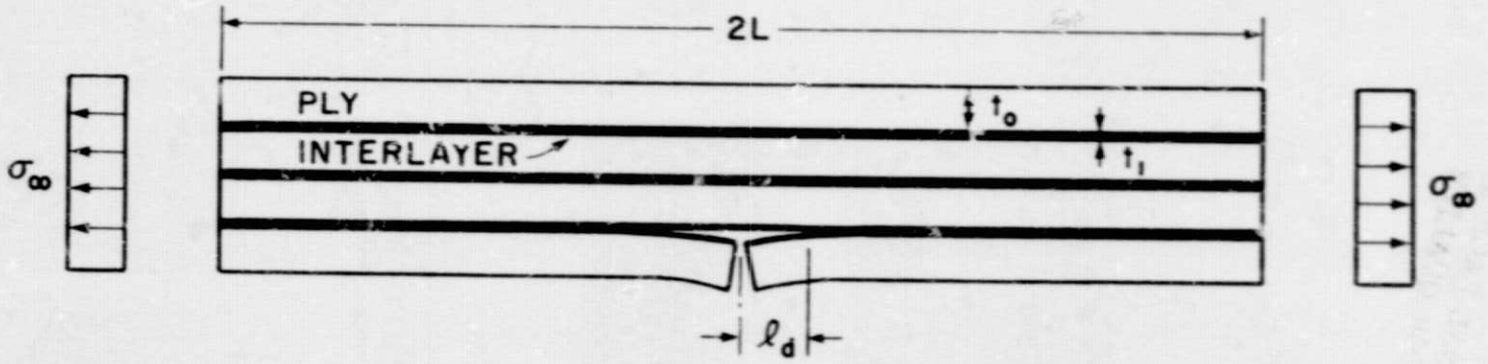

(a) Geometry ($L = 20t_o = 200\ t_1$)

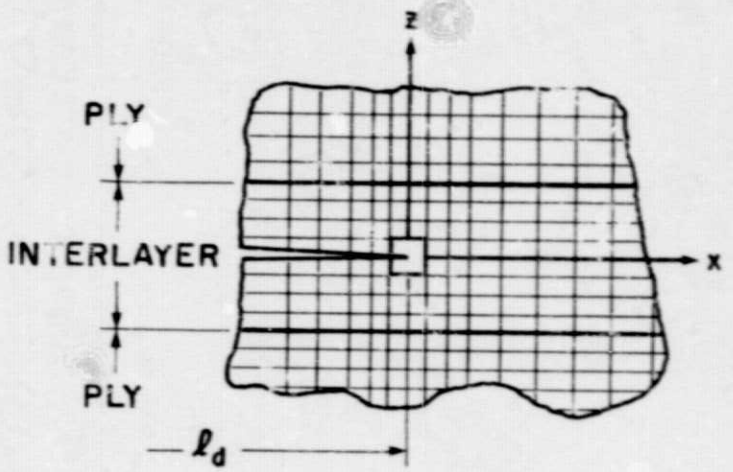

(b) Finite Element Mesh near delamination crack tip

FIGURE 2.

DELAMINATION CRACK GEOMETRY AND FINITE ELEMENT MESH NEAR DELAMINATION CRACK TIP.

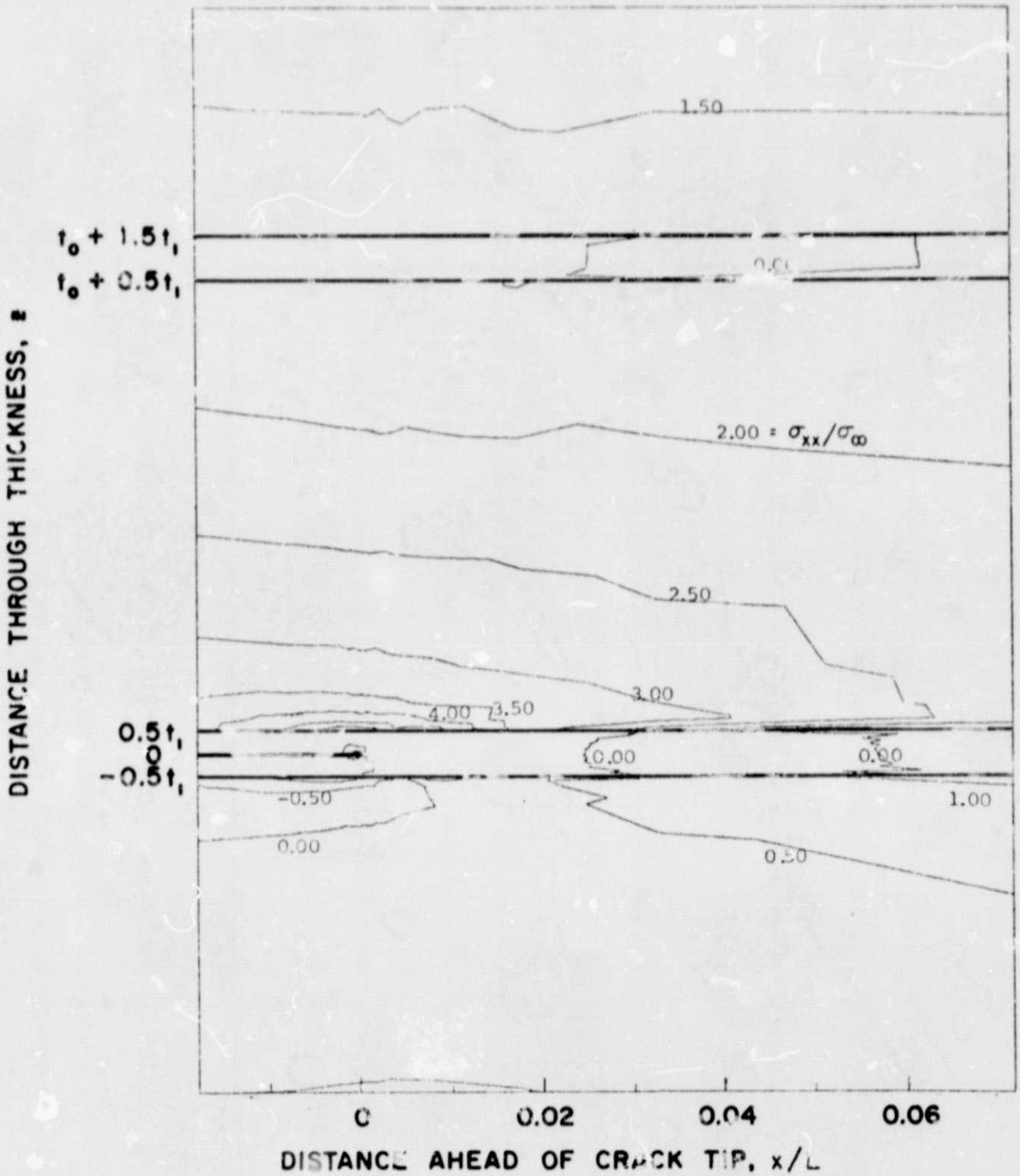

FIGURE 3.

LONGITUDINAL STRESS CONTOURS ($\sigma_{xx}/\sigma_\infty$) NEAR DELAMINATION CRACK TIP IN 0/0/0/0 GRAPHITE/EPOXY.

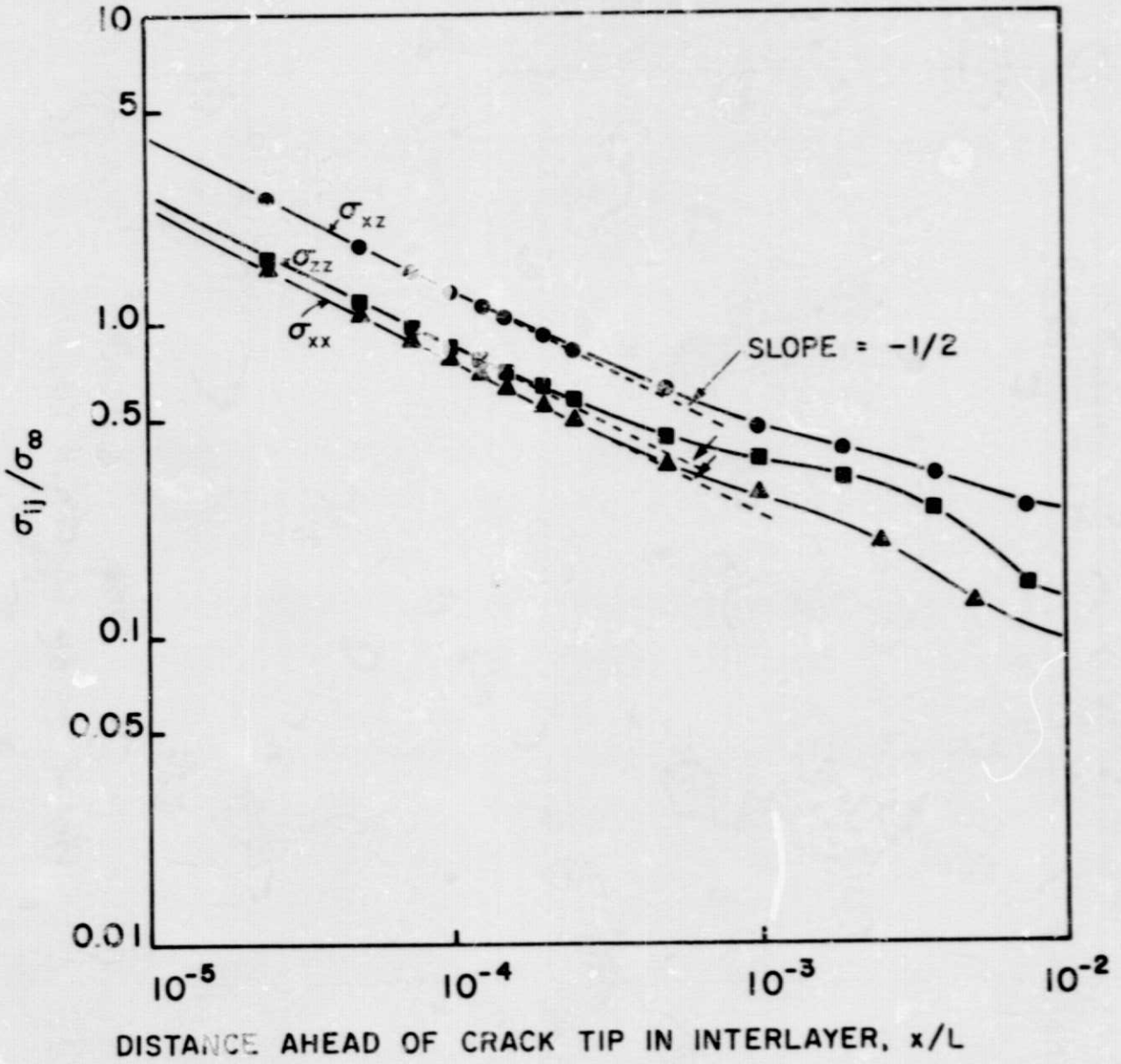

FIGURE 4.

STRESSES AHEAD OF DELAMINATION CRACK TIP IN 0/0/0/0 GRAPHITE/EPOXY COMPOSITE.

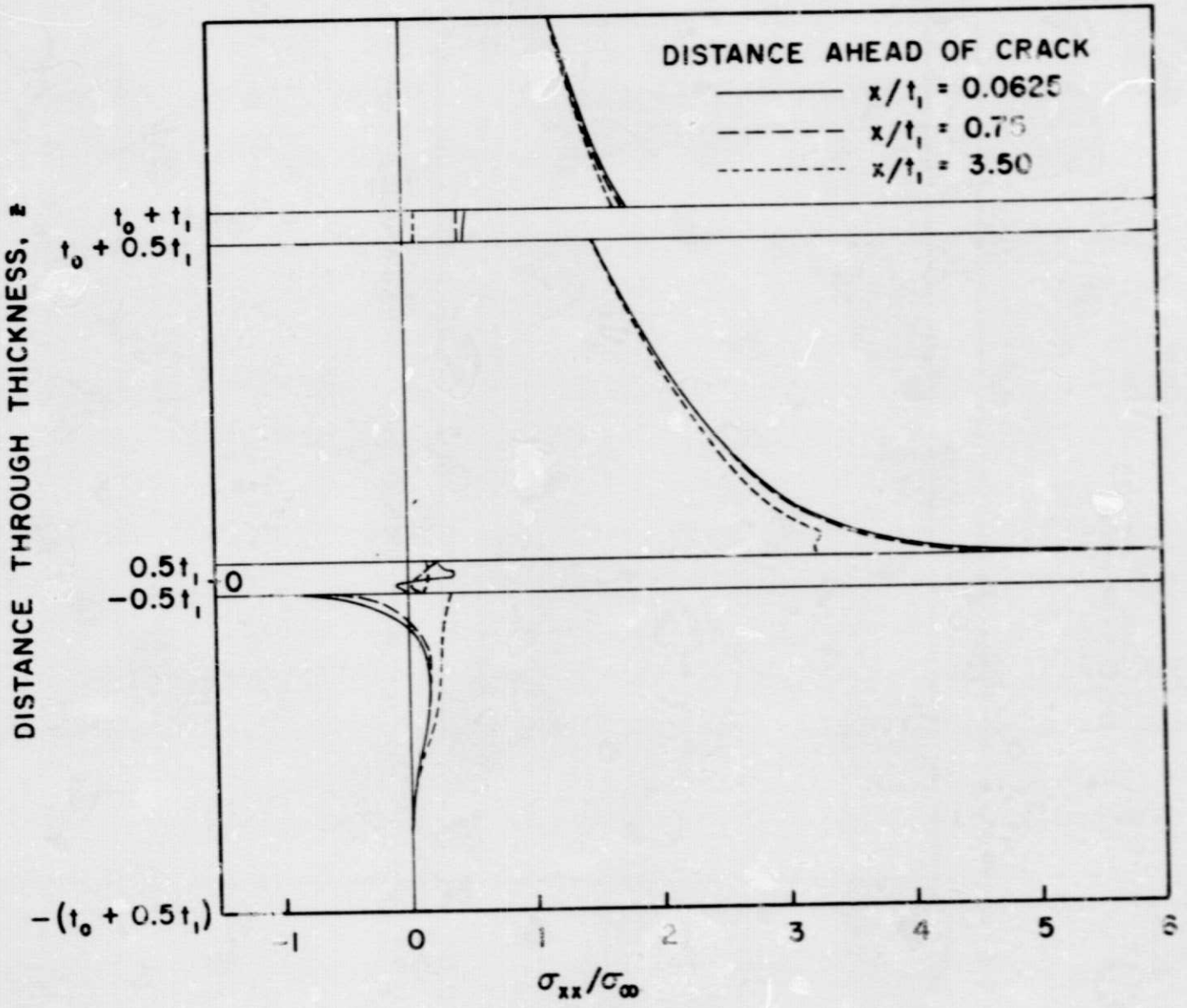

FIGURE 5.

LONGITUDINAL STRESS THROUGH LAMINATE THICKNESS AHEAD OF DELAMINATION CRACK IN 0/0/0/0 GRAPHITE EPOXY.

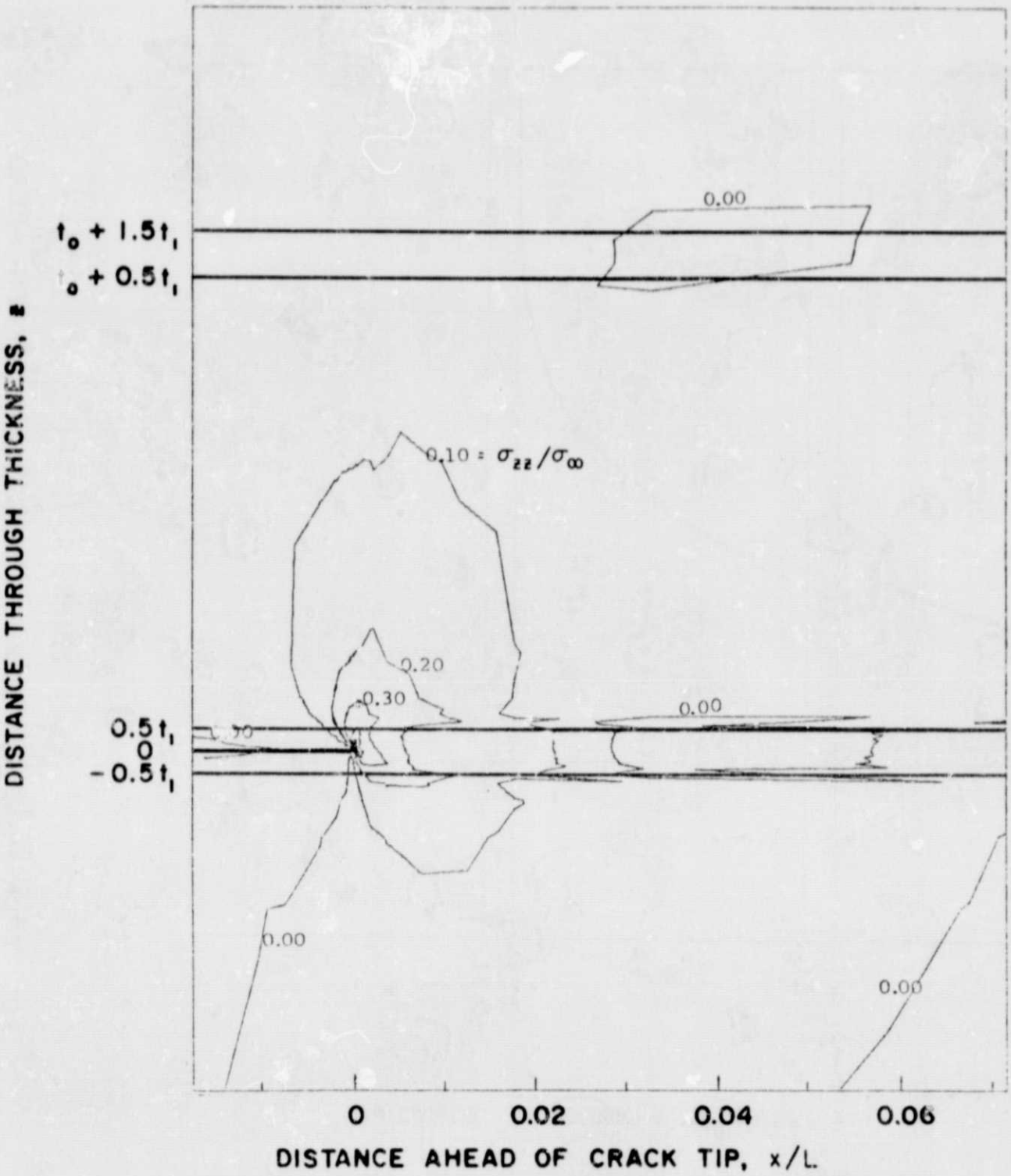

FIGURE 6.

TRANSVERSE NORMAL STRESS CONTOURS ($\sigma_{zz}/\sigma_\infty$) NEAR DELAMINATION CRACK TIP IN 0/0/0/0 GRAPHITE/EPOXY.

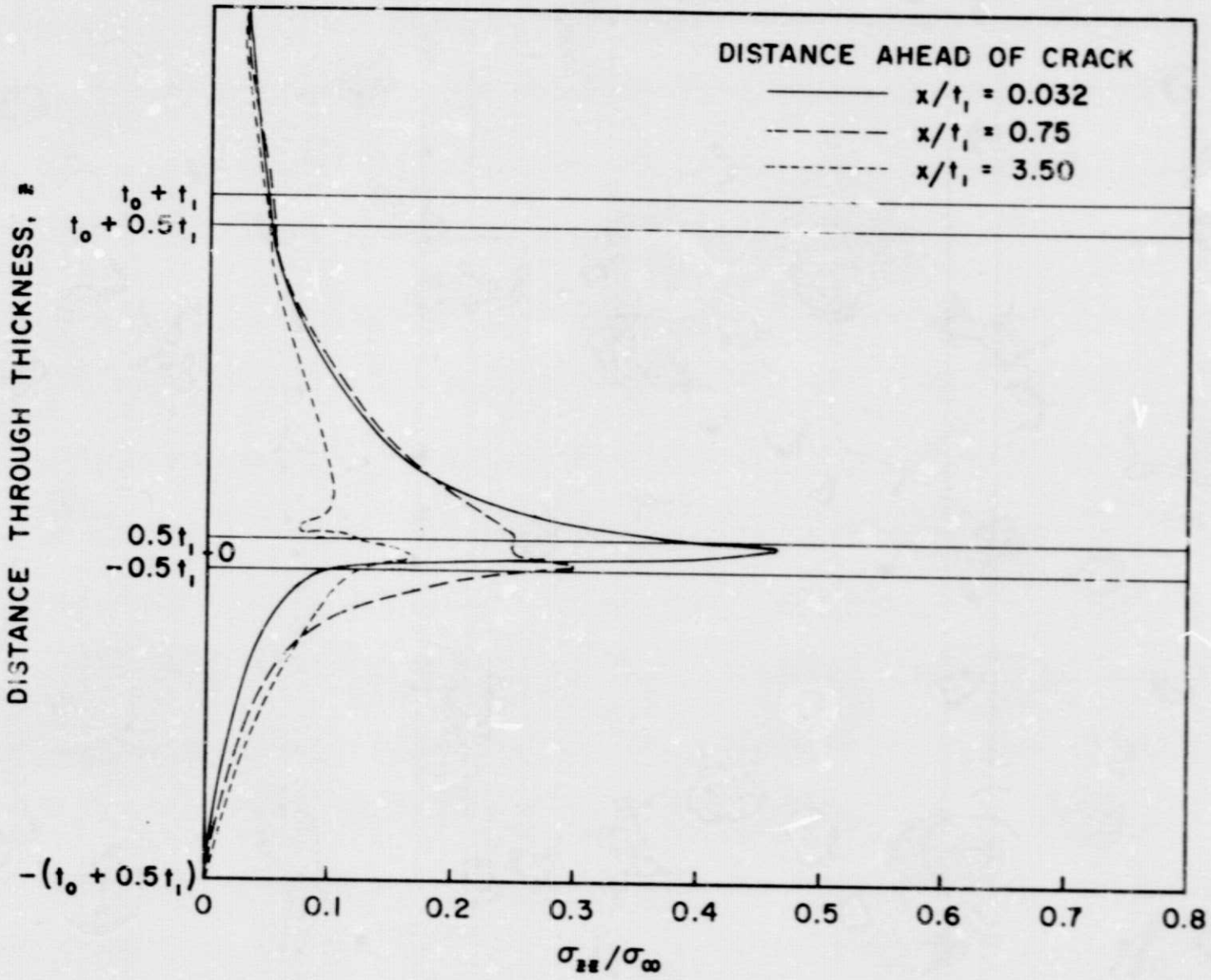

FIGURE 7.

TRANSVERSE NORMAL STRESS THROUGH LAMINATE THICKNESS AHEAD OF DELAMINATION CRACK IN [0/0/0/0] GRAPHITE/EPOXY.

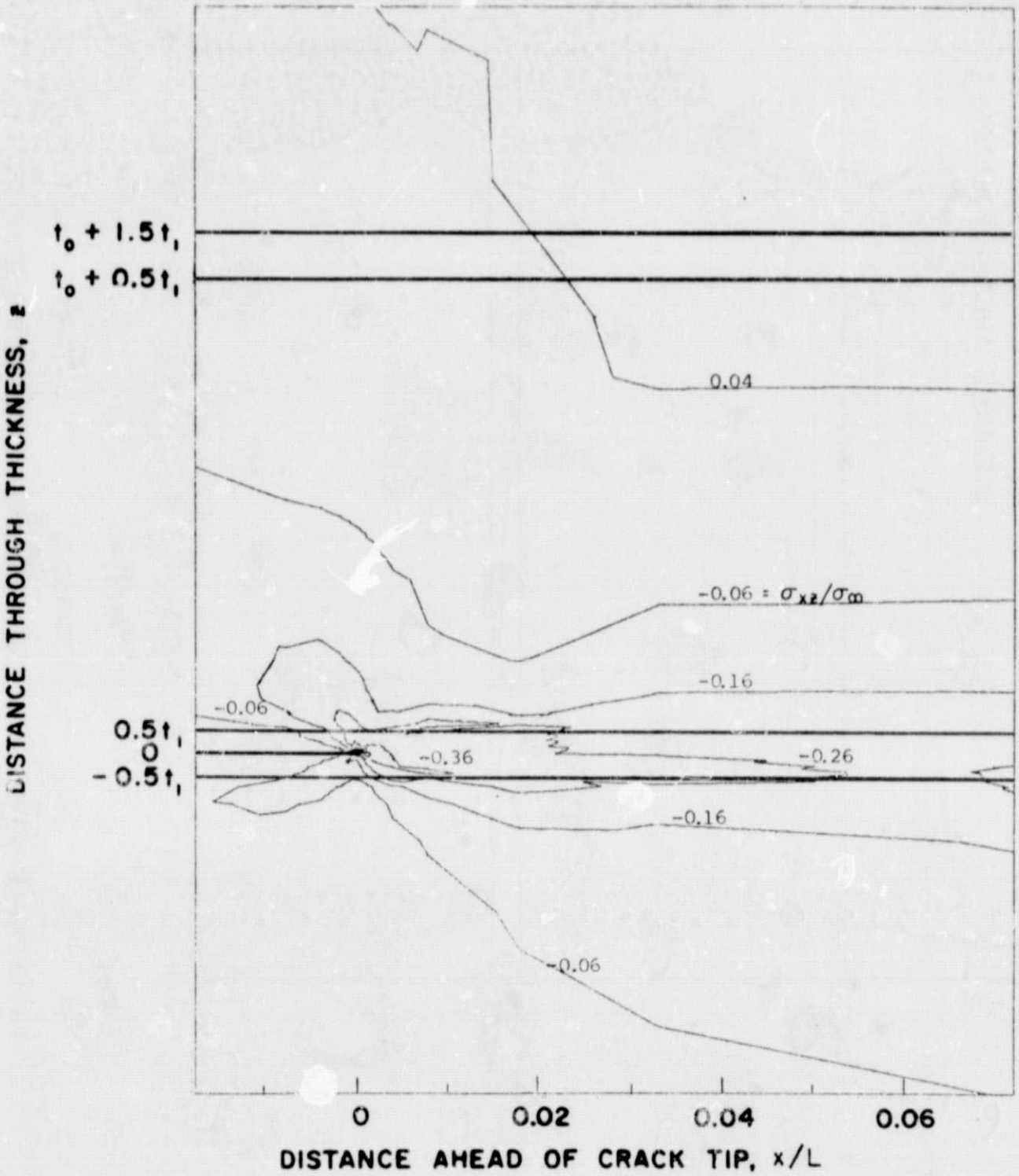

FIGURE 8.

INTERLAMINAR SHEAR STRESS CONTOURS ($\sigma_{xz}/\sigma_\infty$) NEAR DELAMINATION CRACK TIP IN 0/0/0/0 GRAPHITE/EPOXY.

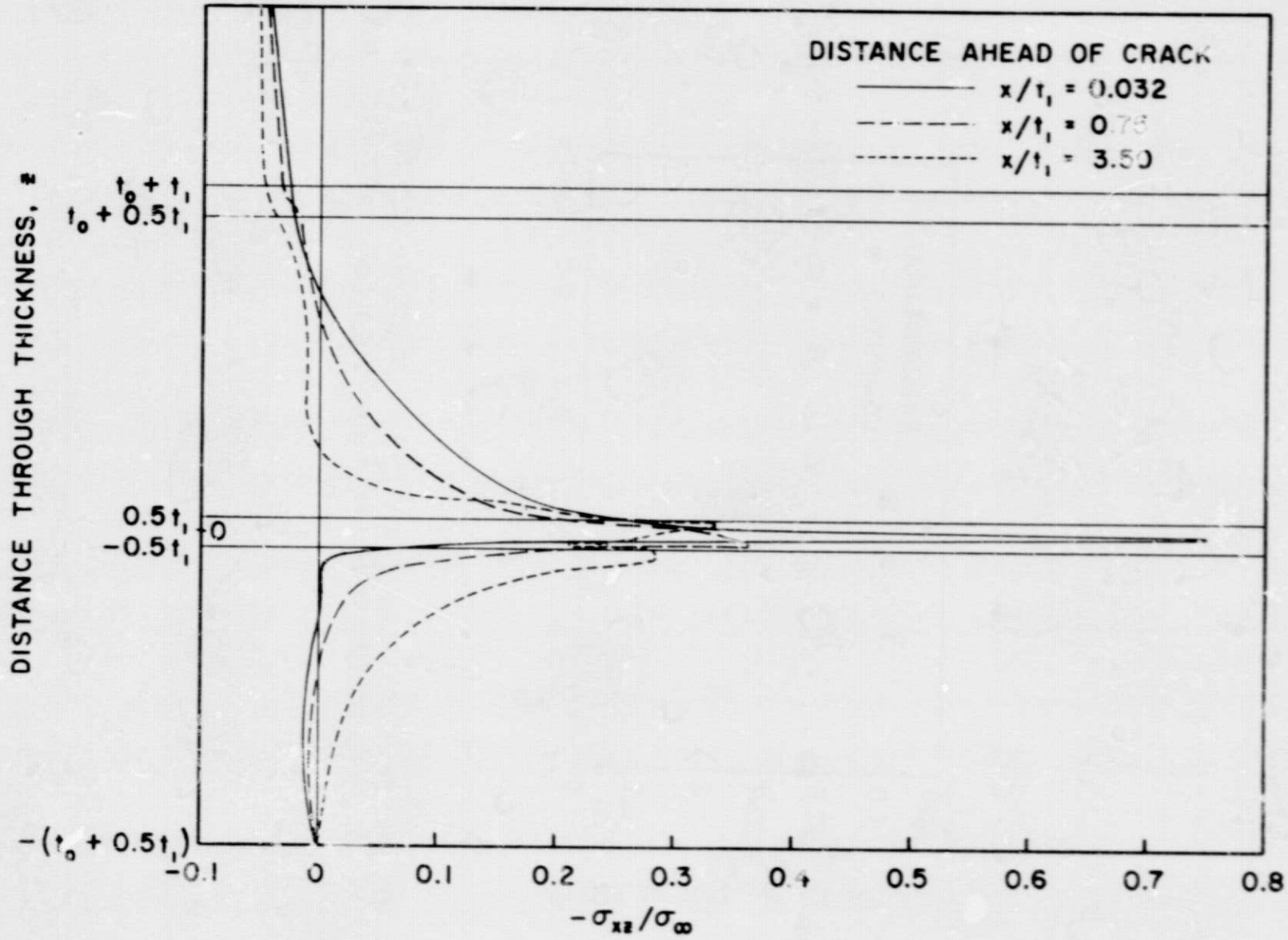

FIGURE 9.

INTERLAMINAR SHEAR STRESS THROUGH LAMINATE THICKNESS AHEAD OF DELAMINATION CRACK IN 0/0/0/0 GRAPHITE/EPOXY.

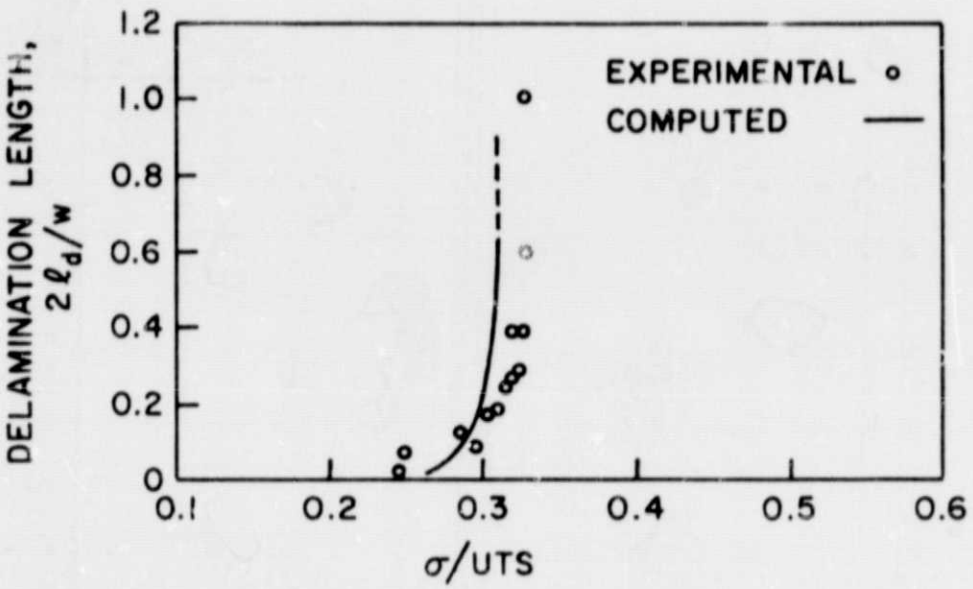

FIGURE 10.

DELAMINATION CRACK GROWTH vs. NOMINAL STRESS.